

# UC Berkeley

## UC Berkeley Previously Published Works

### Title

Characterizing and Understanding the Remarkably Slow Basis Set Convergence of Several Minnesota Density Functionals for Intermolecular Interaction Energies

### Permalink

<https://escholarship.org/uc/item/9rj1t5h8>

### Journal

Journal of Chemical Theory and Computation, 9(10)

### ISSN

1549-9618

### Authors

Mardirossian, Narbe  
Head-Gordon, Martin

### Publication Date

2013-10-08

### DOI

10.1021/ct400660j

Peer reviewed

# Characterizing and understanding the remarkably slow basis set convergence of several Minnesota density functionals for intermolecular interaction energies

Narbe Mardirossian<sup>†</sup> and Martin Head-Gordon<sup>\*,†</sup>

*Department of Chemistry, University of California, Berkeley, and Chemical Sciences Division, Lawrence Berkeley National Laboratory, Berkeley, CA 94720 USA*

E-mail: mhg@cchem.berkeley.edu

## Abstract

For a set of eight equilibrium intermolecular complexes, it is discovered that the basis set limit (BSL) cannot be reached by aug-cc-pV5Z for three of the Minnesota density functionals: M06-L, M06-HF, and M11-L. In addition, the M06 and M11 functionals exhibit substantial, but less severe, difficulties in reaching the BSL. By using successively finer grids, it is demonstrated that this issue is not related to the numerical integration of the exchange-correlation functional. In addition, it is shown that the difficulty in reaching the BSL is not a direct consequence of the structure of the augmented functions in Dunning’s basis sets, since modified augmentation yields similar results. By using a very large custom basis set, the BSL appears to be reached for the HF dimer for all of the functionals. As a result, it is concluded that the difficulties faced by several of the Minnesota density functionals are related to an interplay between the form of these functionals and the structure of standard basis sets. It is speculated that the difficulty in reaching the basis set limit is related to the magnitude of the inhomogeneity correction factor (ICF) of the exchange functional. A

simple modification of the M06-L exchange functional that systematically reduces the basis set superposition error (BSSE) for the HF dimer in the aug-cc-pVQZ basis set is presented, further supporting the speculation that the difficulty in reaching the BSL is caused by the magnitude of the exchange functional ICF. Finally, the BSSE is plotted with respect to the internuclear distance of the neon dimer for two of the examined functionals.

## 1 Introduction

Density functional theory<sup>1,2</sup> is the most widely used computational quantum chemistry method today. Recently, density functionals that can more accurately describe noncovalent interactions have been gaining popularity in many areas of computational chemistry, since the alternative to DFT is wavefunction methods like CCSD(T) that can be prohibitively expensive for large systems. Furthermore, while methods like CCSD(T) tend to require calculations near the basis set limit to provide accurate results,<sup>3</sup> most density functionals perform well with smaller basis sets<sup>4</sup> (typically triple-zeta). In addition, density functionals can be trained with counterpoise corrections<sup>5</sup> for intermolecular interactions ( $\omega$ B97X and  $\omega$ B97X-D),<sup>6,7</sup> or without them. Ultimately, in order to achieve the best results with a semi-empirical density functional, it is important to use it as trained, namely, in a basis set

<sup>\*</sup>To whom correspondence should be addressed

<sup>†</sup>Department of Chemistry, University of California, Berkeley

<sup>‡</sup>Chemical Sciences Division, Lawrence Berkeley National Laboratory, Berkeley, CA 94720 USA

similar to the training basis set and with/without counterpoise corrections. Nonetheless, it is expected that all density functionals have a systematically approachable basis set limit. The BSL can be reached by performing calculations in increasingly larger basis sets with and without counterpoise corrections and assuring that the difference (the BSSE) converges monotonically to zero. The performance of a functional at the basis set limit is arguably the best measure of its quality and accuracy.

## 2 Computational Details

The equations<sup>5</sup> required to counterpoise correct (CP) the binding energy (noCP) of dimer AB are:

$$E_{bind}^{CP}(AB) = E_{AB}^{AB}(AB) - E_{AB}^{AB}(A) - E_{AB}^{AB}(B) \quad (1)$$

$$E_{bind}^{noCP}(AB) = E_{AB}^{AB}(AB) - E_A^A(A) - E_B^B(B) \quad (2)$$

$$E_{BSSE} = E_{bind}^{CP}(AB) - E_{bind}^{noCP}(AB) \quad (3)$$

where the superscripts indicate the basis set, the subscripts indicate the geometry, and the system is in parentheses. Basis set superposition errors for eight intermolecular complexes (Figure 1) were computed for sixteen functionals in the aug-cc-pVXZ<sup>8,9</sup> (X = D, T, Q, 5) [aXZ] family of basis sets. The geometries for the eight dimers were taken from the NCCE31 database<sup>10,11</sup> of Zhao and Truhlar, which are optimized at the MC-QCISD/3 level.<sup>12,13</sup> An integration grid of 99 radial points and 590 angular points was used to evaluate the exchange-correlation components of all of the density functionals. All of the calculations were performed with a development version of Q-Chem 4.0.<sup>14</sup>

## 3 Results

### 3.1 Introduction of the BSSE Issue

In order to introduce the issue at hand, the binding energies of eight intermolecular complexes were analyzed with sixteen density functionals and four basis sets. Table 1 contains the average basis set superposition errors (BSSE) in each basis set, while Table 2 contains the basis set superposition errors (BSSE) and binding energies

(noCP) specifically for the HF dimer. Tables of the same nature as Table 2 can be found in the Supporting Information for the other seven molecules. First, a representative functional from each of the first four rungs of Jacob’s ladder<sup>15</sup> is considered. GVWN<sup>16,17</sup> (Gaspar-Kohn-Sham exchange and VWN correlation) is a functional from the lowest rung (LDA)<sup>18</sup> and has an average BSSE of 0.04 kcal/mol in the aQZ basis set and 0.02 kcal/mol in the a5Z basis set. For PBE,<sup>19</sup> a GGA functional from Rung 2, the average BSSE at aQZ is only 0.03 kcal/mol and 0.01 kcal/mol at a5Z. Representing the meta-GGA functionals on Rung 3 is TPSS,<sup>20</sup> with an average BSSE of 0.02 kcal/mol at aQZ and 0.01 kcal/mol at a5Z. Finally, B3LYP,<sup>21</sup> a hybrid GGA functional from Rung 4, has an average BSSE of 0.03 kcal/mol at aQZ and 0.01 kcal/mol at a5Z. It is very clear from these statistics that for these four functionals, the binding energies are nearly converged in the aQZ basis set and fully converged in the a5Z basis set. For  $\omega$ B97X,<sup>6</sup> the average BSSE at aQZ is 0.04 kcal/mol and the average BSSE at a5Z is 0.02 kcal/mol. Thus, even for a functional with five times more parameters than B3LYP, the binding energies are nearly converged by aQZ. Ultimately, the BSSE for these five functionals converges as expected.

**Table 1: Average basis set superposition errors (BSSE) of eight intermolecular interactions in the aug-cc-pVXZ (X = D, T, Q, 5) [aXZ] basis sets for all of the functionals considered in this paper.**

kcal/mol	Average BSSE			
Functional	aDZ	aTZ	aQZ	a5Z
GVWN	0.34	0.10	0.04	0.02
PBE	0.34	0.06	0.03	0.01
TPSS	0.35	0.09	0.02	0.01
B3LYP	0.33	0.06	0.03	0.01
$\omega$ B97X	0.31	0.06	0.04	0.02
M05	0.35	0.10	0.07	0.07
M05-2X	0.32	0.11	0.06	0.05
M06-L	0.30	0.25	0.34	0.28
M06	0.33	0.19	0.19	0.15
M06-2X	0.32	0.10	0.04	0.04
M06-HF	0.49	0.40	0.35	0.51
M08-HX	0.39	0.24	0.13	0.09
M08-SO	0.35	0.18	0.14	0.08
M11-L	0.43	0.46	0.30	0.18
M11	0.38	0.34	0.25	0.13
VSXC	0.36	0.07	0.03	0.02

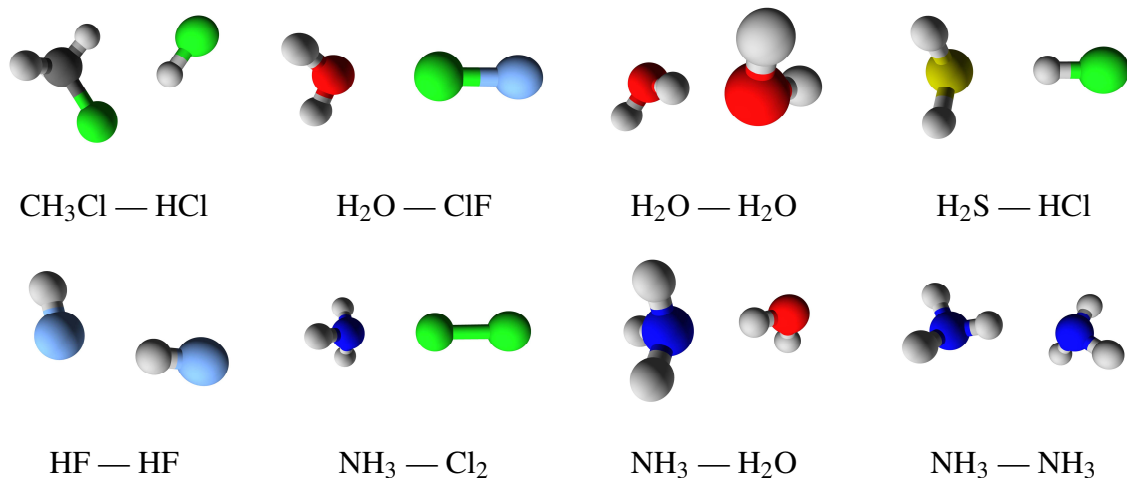


Figure 1: The eight intermolecular complexes analyzed in this paper.

**Table 2: Basis set superposition errors (BSSE) and binding energies (noCP) for HF — HF in the aug-cc-pVXZ (X = D, T, Q, 5) [aXZ] basis sets for all of the functionals considered in this paper.**

kcal/mol Functional	BSSE				noCP			
	aDZ	aTZ	aQZ	a5Z	aDZ	aTZ	aQZ	a5Z
GVWN	0.22	0.11	0.05	0.01	-7.17	-7.11	-7.10	-7.07
PBE	0.20	0.07	0.04	0.01	-4.71	-4.61	-4.65	-4.63
TPSS	0.18	0.12	0.04	0.01	-4.22	-4.16	-4.15	-4.14
B3LYP	0.21	0.07	0.04	0.01	-4.52	-4.43	-4.46	-4.43
$\omega$ B97X	0.19	0.07	0.06	0.02	-5.19	-5.14	-5.14	-5.10
M05	0.23	0.11	0.07	0.07	-5.28	-4.99	-4.94	-4.96
M05-2X	0.19	0.11	0.07	0.07	-4.98	-5.06	-5.03	-5.04
M06-L	0.13	0.17	0.40	0.38	-4.32	-4.46	-4.64	-4.59
M06	0.17	0.15	0.24	0.27	-4.53	-4.40	-4.41	-4.44
M06-2X	0.17	0.11	0.07	0.06	-4.90	-4.95	-4.89	-4.87
M06-HF	0.22	0.44	0.29	1.03	-4.51	-4.71	-4.51	-5.24
M08-HX	0.20	0.26	0.21	0.14	-4.85	-4.94	-4.80	-4.74
M08-SO	0.19	0.15	0.21	0.11	-4.96	-4.74	-4.85	-4.74
M11-L	0.53	0.35	0.28	0.12	-3.81	-3.86	-3.71	-3.41
M11	0.16	0.31	0.42	0.13	-4.53	-4.58	-4.77	-4.47
VSXC	0.23	0.08	0.04	0.01	-4.52	-4.18	-4.20	-4.26

The next ten functionals that will be considered are all Minnesota functionals, namely M05,<sup>22</sup> M05-2X,<sup>23</sup> M06-L,<sup>24</sup> M06,<sup>25</sup> M06-2X,<sup>25</sup> M06-HF,<sup>26</sup> M08-HX,<sup>27</sup> M08-SO,<sup>27</sup> M11-L,<sup>28</sup> and M11.<sup>29</sup> These ten functionals can be separated into three categories based on the severity of their BSSE at the a5Z basis set level: 1). mild (less than 1.5% of noCP on average): M05 (1.5%), M05-2X (1%), M06-2X (0.8%), 2). moderate (between 1.5% and 5% of noCP on average): M06 (3.6%), M08-HX (2%), M08-SO (1.8%), M11 (3.6%), and 3). severe (greater than 5% of noCP on average): M06-L (6.4%), M06-HF (12.1%), M11-L (5.2%). For comparison, the corresponding percentages for the first five functionals considered were 0.2% (GVWN), 0.3% (PBE), 0.4% (TPSS), 0.2% (B3LYP), and 0.4% ( $\omega$ B97X). Finally, the sixteenth functional that is considered is VSXC,<sup>30</sup> mainly because it appears in the functional form of several of the Minnesota functionals. For VSXC, the average BSSE at aQZ is 0.03 kcal/mol and the average BSSE at a5Z is 0.02 kcal/mol with a corresponding percentage of 0.4%. The VSXC results are included to show that the inclusion of the VSXC exchange functional form in M06-L, M06, and M06-HF does not cause this issue.

It is informative to take a closer look at the convergence of the BSSE for the sixteen functionals considered. Picking the HF dimer as the example (Figure 2), it is clear that a majority of the Minnesota functionals have large BSSEs at a5Z. Furthermore, the BSSE for some of the Minnesota

functionals does not decrease monotonically as the basis set size is increased. As expected, the group of functionals with the smallest BSSE at a5Z (#1) is GVWN, PBE, TPSS, B3LYP,  $\omega$ B97X, and VSXC. The BSSE for these functionals decreases monotonically from aDZ to a5Z and is less than 0.02 kcal/mol at a5Z. The next group of functionals (#2) with slightly larger BSSE at a5Z is comprised of M05, M05-2X, and M06-2X. It is no coincidence that these were the three functionals that were previously characterized as having mild BSSE based on their average BSSE for all eight intermolecular interactions. The BSSE for these functionals decreases monotonically as the basis set size is increased, but it appears that going from aQZ to a5Z affords no considerable improvement. The next group of functionals (#3) has between 0.1 – 0.15 kcal/mol of BSSE at a5Z. This group consists of M08-HX, M08-SO, M11-L, and M11. Besides the BSSE at a5Z being quite large for these functionals, it also jumps around between aDZ and a5Z instead of decreasing monotonically. Finally, the last group of functionals includes M06-L, M06, and M06-HF. The most shocking result is the BSSE of M06-HF at a5Z (1.03 kcal/mol). Furthermore, it appears that these three functionals have more BSSE at a5Z than at aDZ! Like the previous group, the BSSE jumps around between aDZ and a5Z. In addition to the HF dimer BSSE at a5Z being unusually large for most of the Minnesota functionals, the BSSE at the aQZ basis set level is shockingly large. For seven of the ten Minnesota functionals, the HF dimer BSSE at aQZ is at least 0.20 kcal/mol, compared to a maximum of 0.07 kcal/mol from the remaining functionals. This is noteworthy because aQZ is generally considered to be close to the basis set limit for most density functionals. However, Figure 2 indicates that the BSSE at aQZ for the HF dimer can be as large as 0.42 kcal/mol for M11. Furthermore, the noCP binding energies change quite drastically between aTZ, aQZ, and a5Z, with values of -4.58 kcal/mol, -4.77 kcal/mol, and -4.47 kcal/mol, respectively, for M11.

### 3.2 Grid

Since it is certainly possible that these issues may be arising from incomplete integration of

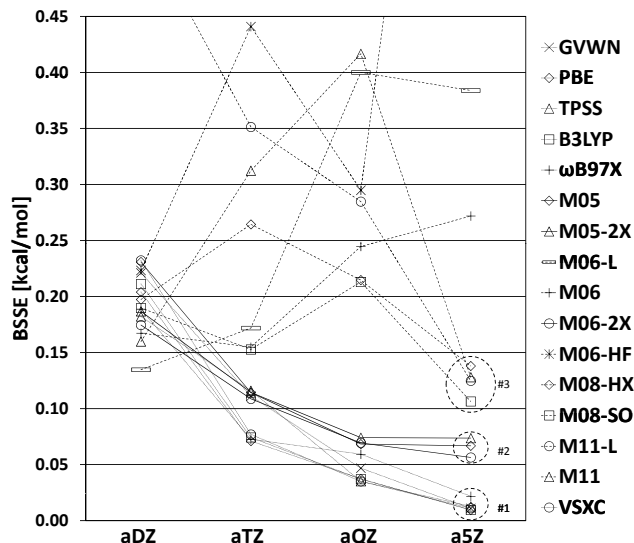


Figure 2: Basis set superposition errors (BSSE) for the HF dimer plotted with respect to the basis set (aug-cc-pVXZ (X = D, T, Q, 5) [aXZ]) for all of the functionals considered in this paper.

the exchange-correlation functional,<sup>31</sup> the effect of changing the grid<sup>32,33</sup> on the BSSE of the HF dimer in the aQZ basis set is shown in Table 3 for the M06-L functional. The column on the right contains the difference between the BSSE value for the (1000,1454) grid and grid shown in the column on the left. This table clearly shows that even when the grid is as fine as 1000 radial points and 1454 angular points, the BSSE persists. Furthermore, the BSSE in the (99,590) grid differs from the BSSE in the (1000,1454) grid by only -0.000054 kcal/mol, implying that the (99,590) results shown in Tables 1 and 2 are converged with respect to the grid.

### 3.3 Reaching the Basis Set Limit

Since it is also possible that the nature of the aug-cc-pVXZ basis sets is responsible for the very slow convergence of some of the Minnesota density functionals, it is worthwhile to investigate several other standard families of basis sets in order to assure that the augmented Dunning basis sets are not at fault. Accordingly, we examined the HF dimer with the maug-cc-pVXZ<sup>34</sup> [maXZ] and cc-pVXZ<sup>8,9</sup> [XZ] (X = D, T, Q) basis sets with eight of the sixteen functionals considered in this paper.

**Table 3: HF dimer basis set superposition errors (BSSE) for the M06-L functional in the aug-cc-pVQZ basis set. The column on the right contains the difference between the BSSE value for the (1000,1454) grid and the grid shown in the column on the left.**

Grid	BSSE [kcal/mol]	Difference [kcal/mol]
SG-0 (23,170)	-0.451711	-0.051680
SG-1 (50,194)	-0.414906	-0.014875
(75,302)	-0.397739	0.002292
(99,590)	-0.400084	-0.000054
(250,590)	-0.400083	-0.000053
(250,974)	-0.400018	0.000012
(250,1454)	-0.400034	-0.000003
(250,5294)	-0.400040	-0.000010
(500,590)	-0.400077	-0.000046
(1000,590)	-0.400083	-0.000053
(2000,590)	-0.400082	-0.000051
(1000,1454)	-0.400030	0.000000

The results, summarized in Table 4, indicate that the removal of the higher angular momentum diffuse basis functions in the maug-cc-pVXZ family does not substantially change the results seen with aug-cc-pVXZ. For PBE, TPSS, and  $\omega$ B97X, the BSSEs at maQZ and aQZ are virtually identical, and the noCP quadruple-zeta binding energies differ at most by 0.04 kcal/mol from the triple-zeta values. However, for the five Minnesota functionals, the difference between the noCP maQZ and noCP maTZ binding energies can be as large as 0.19 kcal/mol for M11-L. Furthermore, the large BSSE still persists at maQZ, ranging from 0.15 kcal/mol to 0.26 kcal/mol. Entirely removing the augmented functions with cc-pVXZ makes it difficult to reach the BSL even for functionals like PBE, TPSS, and  $\omega$ B97X, which did not exhibit difficulties with the aug-cc-pVXZ sequence. These results indicate that augmented basis functions are necessary to reach the BSL for systems with interactions similar to the HF dimer. Ultimately, we conclude that straightforward changes to the established Dunning augmented basis sets are not a viable solution to approaching the complete basis set limit with the Minnesota functionals.

To further pursue results with the Minnesota functionals that approach the basis set limit (which is certainly very difficult to reach), a custom (even-tempered) basis set with 27 s functions, 27 p functions, and 27 d functions was generated and used with the HF dimer (243 basis functions per atom).

The basis set was created by starting with an exponent of 100,000 and dividing by 2 until the exponent was smaller than 0.001. The same basis set was used for both hydrogen and fluorine and all of the basis functions were deliberately chosen to be uncontracted. The results from this basis set are shown in Table 5. With the custom basis set, the BSL for all of the functionals considered in this paper can be closely approached.

For the functionals that are not affected by this issue, the CP and noCP binding energies in the custom basis set are basically identical to the a5Z ones. For example, for B3LYP, the CP and noCP binding energies in the custom basis set are -4.43 kcal/mol and -4.44 kcal/mol, respectively, while in the a5Z basis set, the corresponding values are -4.43 kcal/mol and -4.43 kcal/mol, respectively.

However, this is not the case for the problematic functionals. In the a5Z basis set, M06-HF has a CP binding energy of -4.20 kcal/mol and a noCP binding energy of -5.24 kcal/mol. However, in the custom basis set, the M06-HF binding energies are -4.16 kcal/mol and -4.18 kcal/mol, respectively. This result also indicates that for M06-HF, the CP a5Z binding energy is closer to the BSL than the noCP a5Z binding energy. The same feature can be seen with M06-L, where the CP binding energy in a5Z is -4.21 kcal/mol, while the noCP binding energy in a5Z is -4.59 kcal/mol. In comparison, the custom basis set binding energy is about -4.16 kcal/mol, indicating that the CP a5Z binding energy is almost at the BSL. In fact, for all of the Minnesota functionals that have moderate or severe BSSE, the CP a5Z binding energy for the HF dimer is much closer to the predicted BSL than the noCP a5Z binding energy.

Taking a closer look at the M06-L data in Tables 1 and 2 (as well as the tables in the Supporting Information), it becomes clear that in some cases, the counterpoise-corrected binding energies are generally converging, while the binding energies are not. For example, for  $\text{NH}_3 - \text{H}_2\text{O}$ , the CP binding energy in both the aQZ and a5Z basis sets is -6.00 kcal/mol, while the noCP binding energy changes from -6.36 kcal/mol to -6.21 kcal/mol between the two basis sets. The same trend can be seen with M06-HF, where for the HF dimer, the CP binding energy in aQZ and a5Z is -4.22 kcal/mol and -4.21 kcal/mol respectively, while the noCP bind-

**Table 4: HF dimer basis set superposition errors (BSSE) and binding energies (noCP) for eight density functionals. Results for three different basis sets are presented: maug-cc-pVXZ [maXZ], aug-cc-pVXZ [aXZ], and cc-pVXZ [XZ] (X = D, T, Q).**

kcal/mol Functional	BSSE			noCP			BSSE			noCP			BSSE			noCP		
	maDZ	maTZ	maQZ	maDZ	maTZ	maQZ	aDZ	aTZ	aQZ	aDZ	aTZ	aQZ	DZ	TZ	QZ	DZ	TZ	QZ
PBE	0.41	0.11	0.04	-4.93	-4.60	-4.64	0.20	0.07	0.04	-4.71	-4.61	-4.65	3.45	1.34	0.59	-8.52	-6.18	-5.35
TPSS	0.42	0.13	0.04	-4.47	-4.11	-4.13	0.18	0.12	0.04	-4.22	-4.16	-4.15	3.10	1.20	0.53	-7.70	-5.53	-4.78
$\omega$ B97X	0.34	0.10	0.05	-5.28	-5.12	-5.11	0.19	0.07	0.06	-5.19	-5.14	-5.14	2.74	0.98	0.40	-8.03	-6.23	-5.56
M06-L	0.41	0.19	0.26	-4.53	-4.48	-4.52	0.13	0.17	0.40	-4.32	-4.46	-4.64	2.17	0.76	0.38	-6.88	-5.31	-4.73
M06	0.43	0.17	0.15	-4.76	-4.43	-4.29	0.17	0.15	0.24	-4.53	-4.41	-4.41	2.66	0.94	0.44	-7.63	-5.50	-4.72
M06-HF	0.36	0.28	0.15	-4.69	-4.47	-4.32	0.22	0.44	0.29	-4.51	-4.71	-4.51	2.93	1.07	0.47	-7.52	-5.47	-4.76
M11-L	0.79	0.32	0.18	-4.05	-3.82	-3.63	0.53	0.35	0.28	-3.81	-3.86	-3.71	1.80	0.87	0.45	-5.68	-4.63	-4.00
M11	0.35	0.23	0.25	-4.72	-4.45	-4.53	0.16	0.31	0.42	-4.53	-4.58	-4.77	3.01	1.01	0.51	-7.84	-5.48	-4.89

ing energy is -4.51 kcal/mol and -5.24 kcal/mol, respectively. Finally, taking a look at the water dimer binding energy for M11, going from noCP aQZ to noCP a5Z takes one from slight overbinding (-5.07 kcal/mol) to moderate underbinding (-4.86 kcal/mol). In comparison, the counterpoise-corrected binding energies in aQZ and a5Z for M11 are -4.77 kcal/mol and -4.76 kcal/mol, respectively.

Since the custom basis set used in this section only had s, p, and d basis functions, the dependence of the BSSE, the CP binding energy, and the noCP binding energy on angular momentum was monitored in Table 6 in order to assure that the actual CBS was approached. The two most diffuse basis functions from the first custom basis set were deleted (to give a total of 25 basis functions of each angular momentum) and calculations were done with 25 s and 25 p basis functions (sp), 25 s, 25 p, and 25 d basis functions (spd), etc., until spdfg. From the data in Table 6, it is clear that the BSL has been approached to  $\sim \pm 0.02$  kcal/mol by spd, with the CP binding energy being -4.16 kcal/mol and the noCP binding energy being -4.18 kcal/mol. Adding 25 f functions per atom only decreases the CP and noCP binding energies by 0.01 kcal/mol. Adding another 25 g functions further decreases the CP binding energy by 0.02 kcal/mol and the noCP binding energy by 0.01 kcal/mol. Thus, it is safe to say that the custom basis set results in Table 5 are indeed approaching the basis set limit to  $\sim \pm 0.02$  kcal/mol in the binding energy. The absolute energies for the custom basis set calculations are also shown in Table 6 for comparison to the a5Z values.

**Table 5: Basis set superposition errors (BSSE), counterpoise-corrected binding energies (CP), and binding energies (noCP) in the first custom basis described in Section 3.3 and aug-cc-pV5Z for the HF dimer for all of the functionals considered in this paper.**

kcal/mol Functional	Custom			aug-cc-pV5Z		
	BSSE	CP	noCP	BSSE	CP	noCP
GVWN	0.00	-7.07	-7.07	0.01	-7.06	-7.07
PBE	0.00	-4.62	-4.63	0.01	-4.62	-4.63
TPSS	0.00	-4.14	-4.14	0.01	-4.13	-4.14
B3LYP	0.00	-4.43	-4.44	0.01	-4.43	-4.43
$\omega$ B97X	0.00	-5.09	-5.10	0.02	-5.08	-5.10
M05	0.04	-4.89	-4.92	0.07	-4.89	-4.96
M05-2X	0.01	-4.99	-5.00	0.07	-4.97	-5.04
M06-L	0.01	-4.16	-4.17	0.38	-4.21	-4.59
M06	0.02	-4.13	-4.15	0.27	-4.17	-4.44
M06-2X	0.01	-4.84	-4.86	0.06	-4.81	-4.87
M06-HF	0.02	-4.16	-4.18	1.03	-4.20	-5.24
M08-HX	0.01	-4.61	-4.61	0.14	-4.60	-4.74
M08-SO	0.02	-4.63	-4.65	0.11	-4.63	-4.74
M11-L	0.01	-3.26	-3.27	0.12	-3.29	-3.41
M11	0.01	-4.29	-4.30	0.13	-4.34	-4.47
VSXC	0.00	-4.23	-4.24	0.01	-4.25	-4.26

**Table 6: Basis set superposition errors (BSSE), counterpoise-corrected binding energies (CP), and binding energies (noCP) in the second custom basis set described in Section 3.3 and aug-cc-pV5Z for the HF dimer for the M06-L functional. The second through sixth rows contain absolute energies in hartrees, while the last three rows are in kcal/mol. ABGhost indicates that ghost basis functions are placed on monomer B, while AGhostB indicates that ghost basis functions are placed on monomer A.**

	a5Z	sp	spd	spdf	spdfg
AB	-200.96453	-200.95646	-200.96990	-200.97079	-200.97104
ABGhost	-100.47890	-100.47472	-100.48165	-100.48211	-100.48224
AGhostB	-100.47892	-100.47465	-100.48161	-100.48207	-100.48221
A	-100.47863	-100.47457	-100.48164	-100.48209	-100.48223
B	-100.47859	-100.47455	-100.48161	-100.48206	-100.48219
BSSE	0.38	0.15	0.01	0.02	0.02
CP	-4.21	-4.45	-4.16	-4.15	-4.13
noCP	-4.59	-4.60	-4.18	-4.17	-4.16

### 3.4 Analysis of the Minnesota Functionals

The DFT exchange components of all of the Minnesota functionals considered in this paper can be described by three main equations. M05, M05-2X, and M06-2X are characterized by Equation 4, M06-L, M06, and M06-HF are characterized by Equation 5, and M08-SO, M08-HX, M11-L, and M11 are characterized by Equation 6. For M11-L and M11, there is an additional multiplicative factor that arises as a result of the range-separation which has been omitted here. In these equations,  $e_{x,\sigma}^{LSDA}$  is the local spin density approximation (LSDA) exchange energy density per unit volume and  $f_{x,\sigma}$  represents inhomogeneity correction factors. During the parameterization of these functionals, the parameters of the PBE and RPBE<sup>35</sup> inhomogeneity correction factors were not optimized, while the parameters of  $f_{x,\sigma}^M$  and  $f_{x,\sigma}^{VSXC}$  were optimized. Since  $f_{x,\sigma}^M$  appears in all of the Minnesota functionals considered here, it is the focus of this paper and its form is described<sup>36</sup> by Equations 7-10. In these equations,  $w_\sigma$  is the transformed local kinetic energy ratio, with a range of  $[-1, 1]$ .

$$E_x^{DFT} = \sum_{\sigma}^{\alpha,\beta} \int e_{x,\sigma}^{LSDA}(\rho_\sigma) [f_{x,\sigma}^{PBE}(\rho_\sigma, \nabla\rho_\sigma) f_{x,\sigma}^M(\rho_\sigma, \tau_\sigma)] d\mathbf{r} \quad (4)$$

$$E_x^{DFT} = \sum_{\sigma}^{\alpha,\beta} \int e_{x,\sigma}^{LSDA}(\rho_\sigma) [f_{x,\sigma}^{PBE}(\rho_\sigma, \nabla\rho_\sigma) f_{x,\sigma}^M(\rho_\sigma, \tau_\sigma) + f_{x,\sigma}^{VSXC}(\rho_\sigma, \nabla\rho_\sigma, \tau_\sigma)] d\mathbf{r} \quad (5)$$

$$E_x^{DFT} = \sum_{\sigma}^{\alpha,\beta} \int e_{x,\sigma}^{LSDA}(\rho_\sigma) [f_{x,\sigma}^{PBE}(\rho_\sigma, \nabla\rho_\sigma) f_{x,\sigma}^{M1}(\rho_\sigma, \tau_\sigma) + f_{x,\sigma}^{RPBE}(\rho_\sigma, \nabla\rho_\sigma) f_{x,\sigma}^{M2}(\rho_\sigma, \tau_\sigma)] d\mathbf{r} \quad (6)$$

$$f_{x,\sigma}^M = \sum_{i=0}^m a_i w_\sigma^i \quad (7)$$

$$w_\sigma = \frac{\frac{\tau_\sigma^{LSDA}}{\tau_\sigma} - 1}{\frac{\tau_\sigma^{LSDA}}{\tau_\sigma} + 1} \quad (8)$$

$$\tau_\sigma^{LSDA} = \frac{3}{10} (6\pi^2)^{2/3} \rho_\sigma^{5/3} \quad (9)$$

$$\tau_\sigma = \frac{1}{2} \sum_i^{occ} |\nabla\psi_{i,\sigma}|^2 \quad (10)$$

Figure 3 plots the exchange functional inhomogeneity correction factors for the 2006 and 2011 Minnesota functionals considered in this paper, while the ICFs for the 2005 and 2008 Minnesota functionals can be found in the Supporting Information. Plots of the Minnesota functional ICFs have appeared previously in the literature (Figure 1 in Reference 28) as a means of examining the ICFs of highly parameterized functionals and assuring that they are well-behaved. It is easily noticeable that in certain regions, the inhomogeneity correction factors of the three functionals that have severe BSSE at a5Z (M06-L, M06-HF, and M11-L) are either much larger than +1 (M06-L and M11-L) or negative (M06-HF). It is important to point out that the ICF for M06-HF goes below zero for a considerable portion of the plot, meaning that grid points that correspond to  $w_\sigma$  values that lie in these regions contribute positive values to the overall exchange energy. According to the plots, positive exchange energies can also occur at certain values of  $w_\sigma$  for M05-2X and M08-HX.

The ICF of M06 (which had an average BSSE of 3.6% at a5Z) also goes well above positive one. Since  $f_{x,\sigma}^M$  multiplies the PBE exchange energy, a horizontal line intersecting the y-axis at  $f_{x,\sigma}^M = 1$  corresponds to the PBE exchange functional, and Figure 3 demonstrates that the Minnesota exchange functionals attempt to correct the PBE exchange energy by increasing its exchange energy contribution at certain values of  $w_\sigma$  and decreasing it at others. Grid points that correspond to specific regions on these plots will be considered in Section 3.5. However, it is important to point out that values of  $w_\sigma = -1$  correspond to exponential tails, while values of  $w_\sigma = 1$  correspond to bond saddle points.<sup>36</sup> Furthermore, the uniform electron gas limit corresponds to  $w_\sigma = 0$ . By looking at the ICFs of these functionals and then considering the BSSE data, it is plausible to conclude that the large magnitude by which the PBE exchange energy is multiplied contributes to the difficulty in reaching the BSL for these functionals.

### 3.5 Modifying M06-L

In order to explore the cause of the difficulty in reaching the basis set limit, the functional form of M06-L was modified in an attempt to reduce the BSSE. This was done by modifying  $f_{x,\sigma}^M$  in Equations 7-8 to  $f_{x,\sigma}^{M'}$  in Equations 11-12 and calculating the CP and noCP binding energies of the HF dimer in the aQZ basis set.

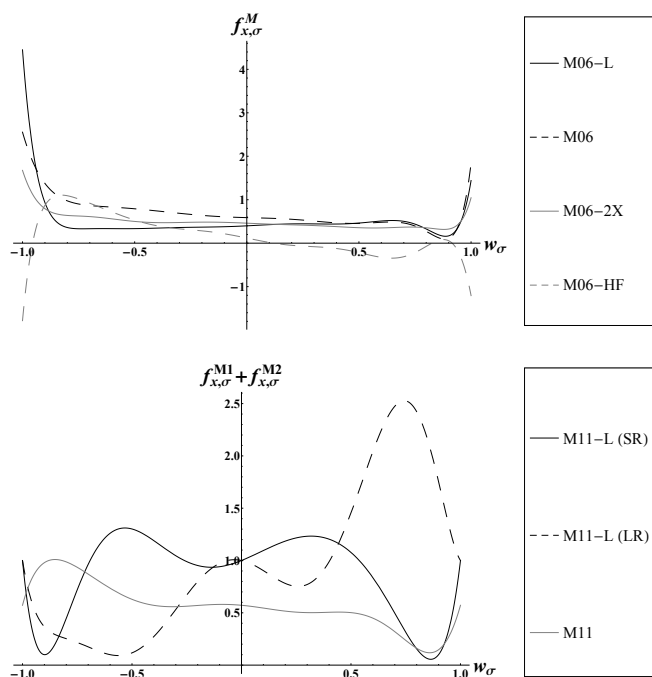


Figure 3: Exchange functional inhomogeneity correction factors for the 2006 Minnesota functionals (top) and the 2011 Minnesota functionals (bottom), plotted as a function of the transformed local kinetic energy ratio,  $w_\sigma$ , defined in Equations 7-10. Plots of the 2005 and 2008 Minnesota functional ICFs can be found in the Supporting Information.

$$f_{x,\sigma}^{M'} = \sum_{i=0}^m a_i w_\sigma^i = \sum_{i=0}^m a_i \left( \frac{\tau_\sigma^{LSDA}}{\tau_\sigma} - (1-a) \right)^i \quad (11)$$

$$f_{x,\sigma}^{M'} = \sum_{i=0}^m a_i w_\sigma^i = \sum_{i=0}^m a_i \left( \frac{(a-1) - \frac{w_\sigma+1}{w_\sigma-1}}{(a+1) - \frac{w_\sigma+1}{w_\sigma-1}} \right)^i \quad (12)$$

Figure 4 shows the effect of changing the parameter,  $a$ , from 0.00 (M06-L) to 0.10 on the exchange functional ICF plot. Table 7 indicates that at  $a = 0.05$ , the BSSE has been reduced by a factor of 6 and is comparable to the BSSE of TPSS at aQZ (0.04 kcal/mol). However, this parameter obviously changes the binding energy as well and is only meant to further show that the culprit is the magnitude by which the PBE exchange energy is being multiplied in certain regions. Although changing the parameter,  $a$ , dramatically reduces the BSSE of M06-L for the HF dimer in the aQZ basis set, it also makes the functional less accurate. At  $a = 0.05$ , while the BSSE is only 0.06 kcal/mol, the binding energy has almost doubled from -4.64 kcal/mol to -8.02 kcal/mol. Thus, there is a trade-off between designing highly accurate (and possibly highly parameterized) functionals and functionals with smooth and well-behaved ICFs.

According to Figure 4 and Table 7, decreasing the magnitude of the ICF in the region corresponding to  $-1.0 \leq w_\sigma \leq -0.5$  gets rid of most of the BSSE. Therefore, in Figure 5, the grid points corresponding to  $-1.0 \leq w_\sigma \leq -0.5$  are shown on the right, and the remaining grid points are shown on the left. These grid points correspond to  $w_\sigma$  values from the final SCF cycle of the M06-L HF dimer calculation. The figure indicates that the region from  $w_\sigma = -0.5$  to  $w_\sigma = 1$  is mainly responsible for *intramolecular* interactions, while the region between  $w_\sigma = -1.0$  and  $w_\sigma = -0.5$  is mainly responsible for *intermolecular* interactions. In the

context of BSSE, it makes sense that modifying  $f_{x,\sigma}^M$  in the region that corresponds to intermolecular interactions leads to a dramatic reduction of the BSSE.

**Table 7: The effect of changing the parameter,  $a$ , described in Equations 11-12 on the basis set superposition error (BSSE) of the HF dimer in the aug-cc-pVQZ basis set for the M06-L functional. The binding energies (noCP) are also shown.**

$a$	BSSE [kcal/mol]	noCP [kcal/mol]
0.00	0.40	-4.64
0.01	0.24	-5.79
0.02	0.15	-6.64
0.03	0.10	-7.27
0.04	0.08	-7.71
0.05	0.06	-8.02
0.06	0.05	-8.23
0.07	0.05	-8.37
0.08	0.05	-8.47
0.09	0.05	-8.53
0.10	0.04	-8.57

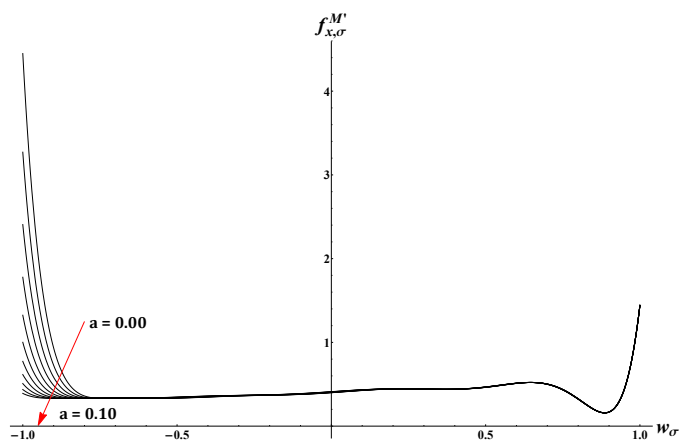


Figure 4: The dependence of the M06-L exchange functional inhomogeneity correction factor on the parameter,  $a$ , described by Equations 11-12. From  $a = 0.00$ , each successive curve is the result of increasing  $a$  by an increment of 0.01, up to the largest considered value of 0.10.

### 3.6 Neon Dimer

As a final exploration of this issue, Figures 6 and 7 show noCP binding energy and BSSE potential energy curves (PEC) for the neon dimer for two of the functionals considered (PBE and M11) in the aDZ, aTZ, aQZ, a5Z, and a6Z basis sets. For the a6Z values, the  $i$  angular momentum basis functions were removed from the basis set. The ref-

erence curve is based on the Tang-Toennies potential model<sup>37</sup> for the neon dimer. All points were evaluated with 500 radial grid points and 974 angular grid points. Taking a look at the PBE binding energies in Figure 6, the only outlier is the noCP aDZ PEC, as expected. The remaining PECs differ from one another by only 0.01 kcal/mol at most, and the equilibrium binding energy ranges from -0.121 kcal/mol (noCP aQZ) to -0.130 kcal/mol (noCP a5Z). Furthermore, the equilibrium distance between the two neon atoms is insensitive to the basis set, remaining consistently around 3.1 Å. For PBE, the magnitude of the BSSE is 1.6% of the noCP binding energy at a5Z on average, while at a6Z, the percentage drops down to only 0.2%. Figure 6 also plots the BSSE of PBE in the same basis sets and it is clear that the BSSE is nonexistent by a5Z and a6Z and less than 0.01 kcal/mol at aQZ. Furthermore, at the equilibrium distance, the BSSE monotonically decreases as the basis set size is increased from aDZ to a6Z.

Figure 7 shows the noCP binding energy and BSSE PECs for one of the newest Minnesota functionals, M11. With this functional, the binding energy ranges all the way from -0.021 kcal/mol (noCP a6Z) to -0.087 kcal/mol (noCP aQZ). Furthermore, the equilibrium distance between the two atoms is very sensitive to the basis set. In the aDZ, a5Z, and a6Z basis sets, this distance is between 3.6 and 3.8 Å, while in the aTZ and aQZ basis sets, it is between 3.1 and 3.3 Å. However, the BSL is reached with the a6Z basis set, with the BSSE being only 1.3% of the noCP binding energy on average. However, at a5Z, this percentage is still very large (28.4%). Also, Figure 7 shows that the BSSE does not decrease with increasing basis set size, but is largest at aQZ, then aTZ, followed by a5Z and aDZ, and finally a6Z. It is alarming that the choice of basis set can have such a dramatic influence on the equilibrium distance of such a simple system, and that the difference between the aQZ and a6Z equilibrium distances can be as large as 0.5 Å for M11.

## 4 Conclusions

This paper explores the performance of sixteen density functionals on eight intermolecular in-

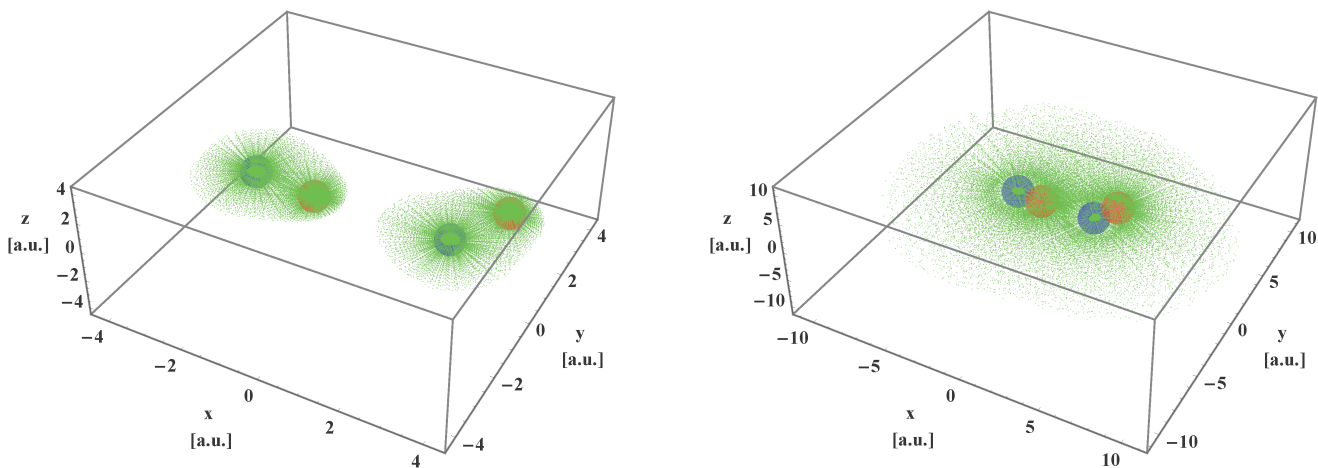


Figure 5: Grid points corresponding to  $-0.5 < w_\sigma \leq 1.0$  (left) and  $-1.0 \leq w_\sigma \leq -0.5$  (right) from a calculation on the HF dimer in the aug-cc-pVQZ basis set with the M06-L functional. The values of  $w_\sigma$  were taken from the final SCF cycle of the calculation. 99 radial points and 590 angular points were used to integrate the exchange-correlation functional.  $w_\sigma$  is described by Equations 7-10. It is evident that  $w_\sigma \in [-1.0, -0.5]$  as shown on the right, corresponds mainly to intermolecular binding, while the remaining grid points correspond to intramolecular binding.

teractions with four commonly used basis sets. GVWN, PBE, TPSS, B3LYP,  $\omega$ B97X, and VSXC have well-defined basis set limits that can be reached by either aug-cc-pVQZ or aug-cc-pV5Z for all eight systems. Of the ten Minnesota functionals considered in this paper, M05, M05-2X, and M06-2X are the best behaved. For these three functionals, the BSSE at aug-cc-pV5Z is about 1% of the binding energy (compared to about 0.3% for the six non-Minnesota functionals considered). For M08-HX and M08-SO, the BSSE at aug-cc-pV5Z is about 2% of the binding energy on average. Finally, for M06-L, M06, M06-HF, M11-L, and M11, the BSSE at aug-cc-pV5Z is at least 3.5% of the binding energy on average, but can be as large as 5.2% for M11-L, 6.4% for M06-L, and 12.1% for M06-HF. Comfortingly, it was shown in Section 3.3 that the basis set limit can be approached for all ten functionals. Furthermore, it was shown in Section 3.2 that this issue is not related to the incomplete integration of the exchange-correlation functional. In addition to the eight intermolecular interactions, potential energy curves for the neon dimer were calculated with PBE and M11. It was found that both the equilibrium binding energy and the equilibrium bond

length for M11 were highly sensitive to the basis set. In fact, it was shown that the difference between the quadruple-zeta-optimized and sextuple-zeta-optimized neon dimer bond length for M11 was as large as 0.5 Å.

Table 8 shows the root-mean-square deviations (RMSD) of all 16 functionals in the aug-cc-pVXZ (X = D, T, Q, 5) basis sets, both with and without counterpoise corrections. The reference values were taken from Zhao and Truhlar’s NCCE31 database.<sup>10,11</sup> The values in bold indicate the smallest error for a given functional, while the underlined values indicate the largest error for a given functional. For eleven of the sixteen functionals, it appears that the counterpoise-corrected aug-cc-pVTZ binding energies provide the best statistics. The ten Minnesota functionals were trained in a triple-zeta basis set, and the column that should contain the best results is the noCP aTZ column. However, even though this is the case only for M06-HF and M11, for most of the remaining Minnesota functionals, the largest deviation between the noCP aTZ error and the actual minimum is less than 0.07 kcal/mol. Thus, it is still valid to claim that these functionals should be most accurate when used in the aug-cc-pVTZ

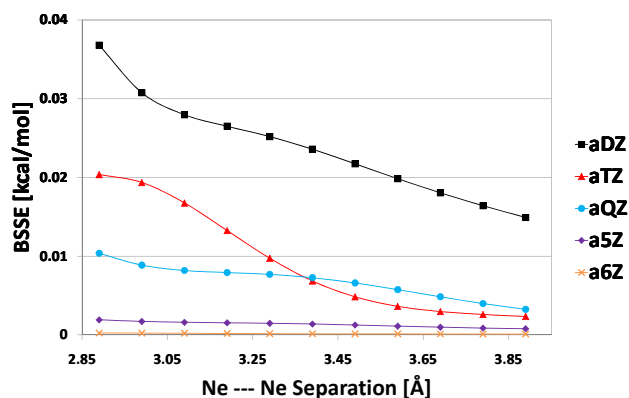
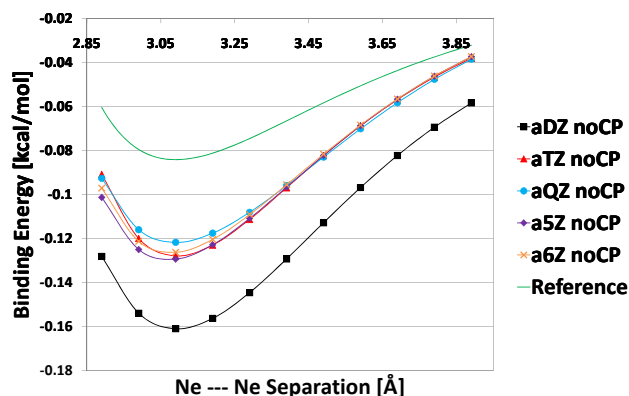


Figure 6: PBE potential energy curves (PEC) for the neon dimer in the aug-cc-pVXZ (X = D, T, Q, 5, 6) basis sets. Binding energy PECs are shown in the top figure, while basis set superposition error PECs are shown in the bottom figure. For the aug-cc-pV6Z values, the  $i$  angular momentum basis functions were removed from the basis set.

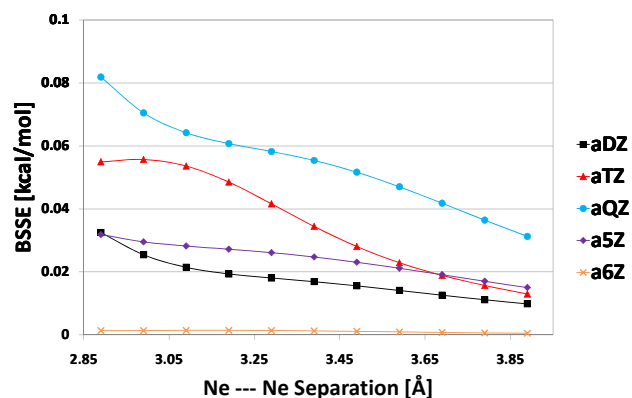
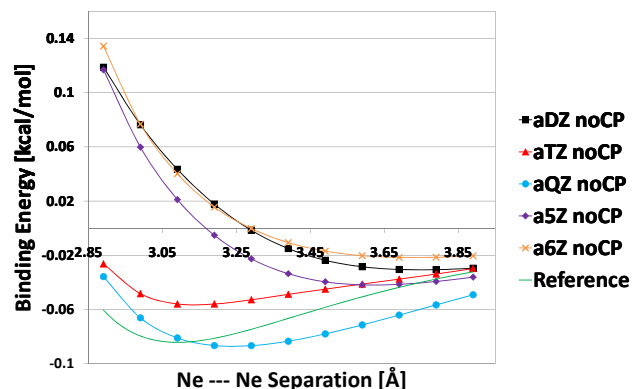


Figure 7: M11 potential energy curves (PEC) for the neon dimer in the aug-cc-pVXZ (X = D, T, Q, 5, 6) basis sets. Binding energy PECs are shown in the top figure, while basis set superposition error PECs are shown in the bottom figure. For the aug-cc-pV6Z values, the  $i$  angular momentum basis functions were removed from the basis set.

basis set without counterpoise corrections. However, although it is true that a density functional should be most accurate when used in conjunction with the basis set that it was parameterized with, there are certainly cases (i.e. systems that were not included in the training set) where this concept might not apply. Therefore, functionals are usually optimized as close to the basis set limit as possible, so that using a basis set *larger* than the training basis set is not detrimental. This idea is definitely conveyed in Table 8, as the worst RMSDs are almost always found in the aDZ column, with the differences between the aTZ, aQZ, and a5Z RMSDs being small.

**Table 8: Root-mean-square deviations (RMSD) for eight intermolecular interactions. CP refers to counterpoise-corrected binding energies and noCP refers to binding energies. Results for sixteen functionals in the aug-cc-pVXZ (X = D, T, Q, 5) [aXZ] basis sets are displayed. The reference values were taken from Truhlar’s NCCE31 database.<sup>10,11</sup> The numbers in bold indicate the smallest RMSD for a given functional and underlined numbers indicate the largest RMSD for a given functional.**

kcal/mol Functional	CP				noCP			
	aDZ	aTZ	aQZ	a5Z	aDZ	aTZ	aQZ	a5Z
GVWN	4.06	<b>3.98</b>	4.01	4.04	<u>4.39</u>	4.07	4.04	4.06
PBE	1.27	<b>1.13</b>	1.16	1.20	<u>1.51</u>	1.17	1.18	1.20
TPSS	1.06	<b>0.93</b>	0.95	0.97	<u>1.19</u>	0.94	0.95	0.97
B3LYP	<u>0.72</u>	0.67	0.66	0.67	<b>0.63</b>	0.64	0.65	0.66
$\omega$ B97X	0.73	<b>0.63</b>	0.63	0.65	<u>1.04</u>	0.69	0.68	0.67
M05	0.50	<b>0.28</b>	0.33	0.34	<u>0.80</u>	0.34	0.37	0.37
M05-2X	0.35	<b>0.32</b>	0.33	0.35	<u>0.58</u>	0.39	0.37	0.38
M06-L	1.18	0.89	<b>0.87</b>	0.88	<u>1.35</u>	0.99	0.95	0.92
M06	0.70	<b>0.44</b>	0.48	0.50	<u>0.90</u>	0.47	0.46	0.48
M06-2X	0.41	<b>0.28</b>	0.29	0.31	<u>0.65</u>	0.34	0.32	0.32
M06-HF	0.36	0.59	<u>0.65</u>	0.63	0.45	<b>0.34</b>	0.47	0.41
M08-HX	0.50	<b>0.23</b>	0.24	0.27	<u>0.85</u>	0.40	0.31	0.31
M08-SO	0.51	<b>0.22</b>	0.24	0.28	<u>0.82</u>	0.33	0.32	0.31
M11-L	1.33	1.01	1.06	1.13	<u>1.35</u>	0.98	<b>0.92</b>	1.05
M11	0.31	<u>0.53</u>	0.52	0.53	0.27	<b>0.22</b>	0.35	0.41
VSXC	1.34	<b>1.28</b>	1.42	1.54	1.54	1.31	1.43	<u>1.55</u>

The main origin of the very slow convergence of M06-L, M06-HF, and M11-L (as well as M06 and M11) toward the complete basis set limit for intermolecular interactions is likely to be the behavior of their exchange functional inhomogeneity correction factors (ICF). Plots showing the dependence of the exchange functional ICF on the transformed local kinetic energy ratio,  $w_{\sigma}$ , reveal two

issues. In M06-HF, the ICF can be negative, which is likely unphysical. Additionally, the ICF can be very large in M06-L as  $w_{\sigma} \rightarrow -1$ , a region important for intermolecular interactions. Modifying M06-L to change this behavior removes its slow convergence of BSSE with basis set. While the many semi-empirical parameters in the Minnesota density functionals are not *directly* responsible for the convergence difficulties observed, the great freedom that such forms permit introduces oscillations into the meta-GGA inhomogeneity correction factors, which appear to be the real cause of the issue. We suggest that such factors should be carefully examined in the development of future density functionals.

## 5 Supporting Information

The inhomogeneity correction factors for the 2005 and 2008 Minnesota functional are included in the Supporting Information. Furthermore, data for the remaining seven molecules in the form of Table 2 is included in the Supporting Information. This information is available free of charge via the Internet at <http://pubs.acs.org/>.

## 6 Acknowledgements

This work was supported by the Director, Office of Energy Research, Office of Basic Energy Sciences, Chemical Sciences Division of the U.S. Department of Energy under Contract DE-AC0376SF00098, and by a grant from the SciDac Program.

## References

- (1) Hohenberg, P.; Kohn, W. *Phys. Rev.* **1964**, *136*, B864–B871.
- (2) Kohn, W.; Sham, L. J. *Phys. Rev.* **1965**, *140*, A1133–A1138.
- (3) Halkier, A.; Helgaker, T.; Jørgensen, P.; Klopper, W.; Koch, H.; Olsen, J.; Wilson, A. K. *Chem. Phys. Lett.* **1998**, *286*, 243–252.
- (4) Boese, A. D.; Martin, J. M. L.; Handy, N. C. *J. Chem. Phys.* **2003**, *119*, 3005–3014.
- (5) Boys, S. F.; Bernardi, F. *Mol. Phys.* **1970**, *19*, 553–566.
- (6) Chai, J.-D.; Head-Gordon, M. *J. Chem. Phys.* **2008**, *128*, 084106.
- (7) Chai, J.-D.; Head-Gordon, M. *Phys. Chem. Chem. Phys.* **2008**, *10*, 6615–6620.
- (8) Woon, D. E.; Dunning Jr., T. H. *J. Chem. Phys.* **1993**, *98*, 1358–1371.
- (9) Dunning Jr., T. H. *J. Chem. Phys.* **1989**, *90*, 1007–1023.
- (10) Zhao, Y.; Truhlar, D. G. *J. Chem. Theory Comput.* **2005**, *1*, 415–432.
- (11) Zhao, Y.; Truhlar, D. G. *J. Phys. Chem. A* **2005**, *109*, 5656–5667.
- (12) Fast, P. L.; Truhlar, D. G. *J. Phys. Chem. A* **2000**, *104*, 6111–6116.
- (13) Lynch, B. J.; Truhlar, D. G. *J. Phys. Chem. A* **2003**, *107*, 3898–3906.
- (14) Shao, Y. et al. *Phys. Chem. Chem. Phys.* **2006**, *8*, 3172–3191.
- (15) Perdew, J. P.; Ruzsinszky, A.; Tao, J.; Staroverov, V. N.; Scuseria, G. E.; Csonka, G. I. *J. Chem. Phys.* **2005**, *123*, 062201.
- (16) Gáspár, R. *Acta Phys. Hung.* **1974**, *35*, 213–218.
- (17) Vosko, S. H.; Wilk, L.; Nusair, M. *Can. J. Phys.* **1980**, *58*, 1200–1211.
- (18) Thomas, L. H. *Proc. Cambridge Philos. Soc.* **1927**, *23*, 542–548.
- (19) Perdew, J. P.; Burke, K.; Ernzerhof, M. *Phys. Rev. Lett.* **1996**, *77*, 3865–3868.
- (20) Tao, J.; Perdew, J. P.; Staroverov, V. N.; Scuseria, G. E. *Phys. Rev. Lett.* **2003**, *91*, 146401.
- (21) Becke, A. D. *J. Chem. Phys.* **1993**, *98*, 5648–5652.
- (22) Zhao, Y.; Schultz, N. E.; Truhlar, D. G. *J. Chem. Phys.* **2005**, *123*, 161103.
- (23) Zhao, Y.; Schultz, N. E.; Truhlar, D. G. *J. Chem. Theory Comput.* **2006**, *2*, 364–382.
- (24) Zhao, Y.; Truhlar, D. G. *J. Chem. Phys.* **2006**, *125*, 194101.
- (25) Zhao, Y.; Truhlar, D. *Theor. Chem. Acc.* **2008**, *120*, 215–241.
- (26) Zhao, Y.; Truhlar, D. G. *J. Phys. Chem. A* **2006**, *110*, 13126–13130.
- (27) Zhao, Y.; Truhlar, D. G. *J. Chem. Theory Comput.* **2008**, *4*, 1849–1868.
- (28) Peverati, R.; Truhlar, D. G. *J. Phys. Chem. Lett.* **2012**, *3*, 117–124.
- (29) Peverati, R.; Truhlar, D. G. *J. Phys. Chem. Lett.* **2011**, *2*, 2810–2817.
- (30) Voorhis, T. V.; Scuseria, G. E. *J. Chem. Phys.* **1998**, *109*, 400–410.
- (31) Johnson, E. R.; Becke, A. D.; Sherrill, C. D.; DiLabio, G. A. *J. Chem. Phys.* **2009**, *131*, 034111.
- (32) Gill, P. M.; Johnson, B. G.; Pople, J. A. *Chem. Phys. Lett.* **1993**, *209*, 506–512.
- (33) Chien, S.-H.; Gill, P. M. W. *J. Comput. Chem.* **2006**, *27*, 730–739.

- (34) Papajak, E.; Leverentz, H. R.; Zheng, J.; Truhlar, D. G. *J. Chem. Theory Comput.* **2009**, *5*, 1197–1202.
- (35) Hammer, B.; Hansen, L. B.; Nørskov, J. K. *Phys. Rev. B* **1999**, *59*, 7413–7421.
- (36) Becke, A. D. *J. Chem. Phys.* **2000**, *112*, 4020–4026.
- (37) Tang, K. T.; Toennies, J. P. *J. Chem. Phys.* **2003**, *118*, 4976–4983.

## 7 For Table of Contents Use Only

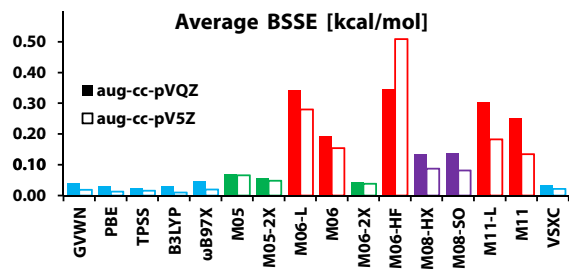


Figure 8: For Table of Contents Use Only